International Conference on Space Optics—ICSO 2008

Toulouse, France

14–17 October 2008

Edited by Josiane Costeraste, Errico Armandillo, and Nikos Karafolas

Opto-mechanical architecture of the LISA instrument

Dennis Weise

Pierangelo Marenaci

Peter Weimer

Marcel Berger

et al.

International Conference on Space Optics — ICSO 2008, edited by Josiane Costeraste, Errico Armandillo, Nikos Karafolas, Proc. of SPIE Vol. 10566, 1056611 · © 2008 ESA and CNES
CCC code: 0277-786X/17/$18 · doi: 10.1117/12.2308192

OPTO-MECHANICAL ARCHITECTURE OF THE LISA INSTRUMENT

Dennis Weise[1], Pierangelo Marenaci[1], Peter Weimer[1], Marcel Berger[1], Hans Reiner Schulte[1], Peter Gath[1], and Ulrich Johann[1]

[1]*EADS Astrium GmbH, Claude-Dornier-Str., 88039 Friedrichshafen, Germany, E-mail: dennis.weise@astrium.eads.net*

ABSTRACT

We report on the latest iteration of the baseline opto-mechanical architecture of the LISA instrument, which has been developed within the current LISA Mission Formulation study under ESA contract. The collective features of the current architecture have been consolidated in an extensive trade of various alternative payload configurations, including variants with only one active proof mass per spacecraft and the application of "In-Field Pointing" for accommodation of constellation breathing.

With respect to the original configuration [1], the newly established architecture most notably distinguishes itself by the use of an off-axis telescope and a "non-frequency-swap" science interferometer for stray light mitigation, as well as the implementation of ancillary pathlength metrology in terms of an "Optical Truss" and Point Ahead Angle sensing.

1. INTRODUCTION

For the detection and characterization of gravitational waves in the frequency range between 30 µHz and 1 Hz, the Laser Interferometer Space Antenna (LISA) will be implemented in a constellation of three identical spacecraft at the corners of an equilateral triangle with a 5 million kilometer arm length, which is trailing Earth in a heliocentric orbit. Each spacecraft carries a payload with two free falling reference cubes, known as "proof masses", defining the end points of the individual arms. The passage of gravitational waves will cause minute changes in the distance between the two proof masses of each arm, which are observed by ultra-sensitive heterodyne laser interferometry, that mutually links the three spacecraft in an active transponder scheme, as illustrated in Figure 1.

Each LISA spacecraft follows its own elliptical orbit around the sun by tracing the inertial motion of the two proof masses on board along their respective sensitive axis with a micronewton propulsion system, which is controlled by the so-called "Drag-Free and Attitude Control System" (DFACS). The resulting spacecraft trajectories form a rotating constellation triangle, whose shape undergoes residual seasonal variations, which cannot be removed completely by orbit optimization, and complicate the accurate determination of arm length fluctuations between them.

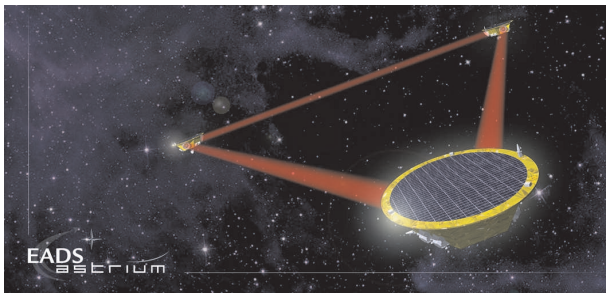

Figure 1. Artist's view of the LISA constellation.

The precision required for the detection of arm length fluctuations is given in terms of the so-called strain sensitivity $h = 2\delta L/L$, for which a noise level on the order of 10^{-20} at a frequency of 5 mHz has to be provided. The detection sensitivity is limited by residual proof mass acceleration from disturbance forces at low frequencies (below 3 mHz), and optical metrology noise at high frequencies (above 3 mHz). In order to comply with the before-mentioned requirement for the strain sensitivity, the total pathlength measurement noise must not exceed

$$12\,\frac{\mathrm{pm}}{\sqrt{\mathrm{Hz}}} \times \sqrt{1+\left(\frac{2.8\,\mathrm{mHz}}{f}\right)^4} \qquad (1)$$

on a single link from one local to its corresponding remote proof mass, where f is the frequency of the spectral noise content.

The optical detection of arm length fluctuations on a single link is separated into two local and one long arm measurement to technically and functionally decouple the inter-spacecraft interferometry from the intra-spacecraft interferometry (Figure 2). This so-

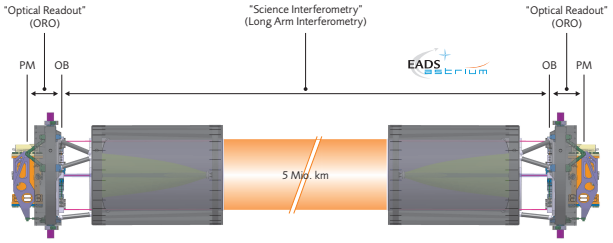

Figure 2. Strap-down architecture. The metrology chain between local and remote proof mass center of mass is separated into three steps, which are combined by on-ground processing on the basis of the dimensional stability of the optical bench.

called "strap-down architecture" had already been introduced by Astrium for earlier payload concepts [1], and is meanwhile fully exploited for the individual optimization of the functional elements in the metrology chain. It is realized by implementing an "Optical Readout" (ORO) for the local detection of proof mass motion with respect to the associated optical bench, and a "science interferometer" that phase-coherently links the local and remote optical bench.

The use of heterodyne interferometry as basic metrology principle in LISA is an intuitive choice, as it naturally combines with the fundamental ideas in General Relativity for establishing scales with light signals, and the unavoidable presence of Doppler shifts on the optical signals received from the remote spacecraft due to their relative motion. The choice of beat frequencies is restricted by the evolution of the relative spacecraft velocities over the duration of the mission, which lead to the necessity to process constantly varying beat notes in a range between 2 and 19 MHz.

Heterodyne interferometry is combined with Differential Wavefront Sensing (DWS) [2, 3] for a highly accurate determination of wavefront tilts in parallel to the longitudinal metrology. This information is required to accomplish a precision pointing/attitude acquisition in order to monitor (if not avoid) the coupling of any line of sight jitter to pathlength noise

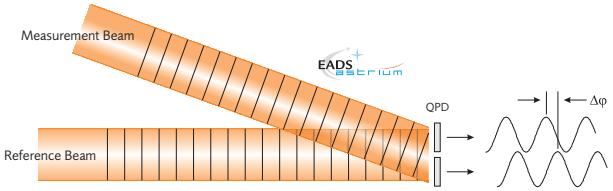

Figure 3. Principle of Differential Wavefront Sensing (DWS). The relative tilt between measurement and reference beam generates a phase shift between the beat notes from different quadrants, from which the angle between the wavefronts can be inferred.

by geometrical crosstalk. DWS is accomplished by performing a spatially resolved phase measurement through the use of quadrant photodiodes in the interferometers, as schematically depicted in Figure 3.

2. OPTO-MECHANICAL CHALLENGES AND CONSTRAINTS

The detection of arm length fluctuations to the required accuracy is complicated by a number of additional challenges and constraints intrinsic to the specifics of the LISA mission. The most prominent of these and their impact on the payload architecture are discussed in the following.

2.1. Breathing Accommodation

The residual seasonal variations in the shape of the constellation triangle not only lead to a variation of the Doppler shifts, as discussed above, but also to changes in the angle between the interferometer arms and in the point-ahead angle. A non-negligible point-ahead between transmitted and received beam in each telescope must be installed due to the relative motion between the spacecraft and the long travel time between them. As illustrated in Figure 4, the typical scale of variations over the mission duration is as follows:

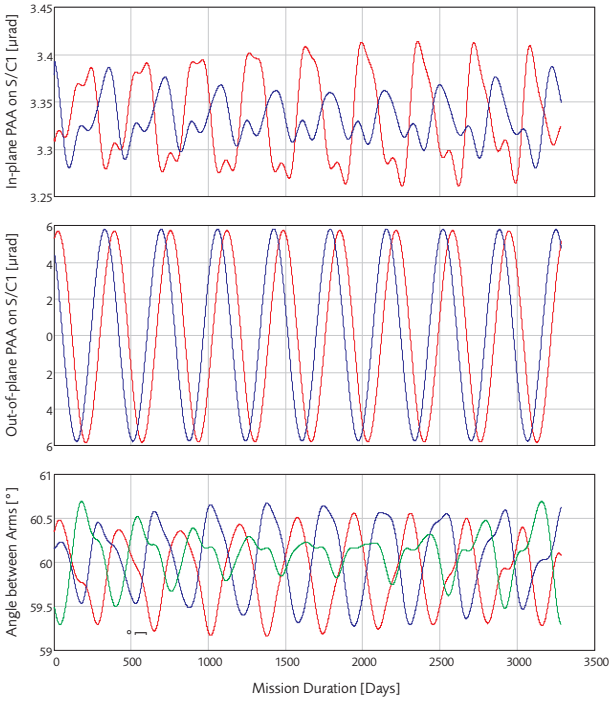

Figure 4. Impact of constellation dynamics on the in-plane and out-of-plane point-ahead angle (top and middle), as well as the angle between the interferometer arms (bottom).

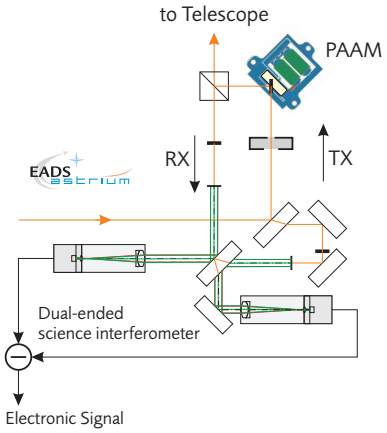

Figure 5. Layout for point ahead adjustment in the transmit path and non-frequency-swap configuration for the science interferometry.

- Angle between interferometer arms: $60^\circ \pm 0.8^\circ$
- In-plane point-ahead angle: $3.35 \pm 0.1\,\mu$rad
- Out-of-plane point-ahead angle: $0 \pm 6\,\mu$rad

An active compensation has to be foreseen for the variation of the angle between the interferometer arms, as well as for the out-of-plane point-ahead angle, since the amplitude exceeds the far field beam width, which is about 3.1 µrad for a telescope diameter of 40 cm.

The baseline approach for adjustment of the out-of-plane point-ahead angle is the implementation of a single axis Gimbal pointing device in a pupil plane of the transmit path, as depicted in Figure 5. Locating this "Point Ahead Angle Mechanism" (PAAM) in the transmit path offers several advantages. Most importantly, avoiding the PAAM in the receive path removes an otherwise significant source of pointing jitter in spacecraft attitude acquisition, which is performed by DWS on the receive beam in the science interferometer. In addition, it allows for a straightforward implementation of an ancillary metrology system to more accurately monitor PAAM pointing jitter and piston noise, by picking off a small portion of the actually transmitted beam behind the PAAM, and mixing it with the local oscillator.

The trade of alternative approaches to accommodate the variation in the angle between the interferometer arms has been the major topic in the recent phase of the LISA Mission Formulation study. A very promising solution that has been suggested and extensively studied by Astrium is known as "In-Field Pointing", where the steering of the individual lines of sight is accomplished by a small actuated mirror inside a specialized wide-field, off-axis telescope. Such a solution would not only permit the implementation of all interferometry of one spacecraft on a single optical bench and thus avoid the need of the so-called backside fiber link for phase referencing of the two active lasers on board, but also is the only identified concept that would enable the realization of a full cold redundancy between two alternative Gravitational Reference Sensor (GRS) systems. It is believed that in consequence, the mission robustness could be crucially improved.

Another option, that has meanwhile been selected by ESA as baseline, is steering the active beam axis of each telescope by rotating an entire assembly of telescope, optical bench, and associated GRS as a whole. In this case, each spacecraft carries two identical Moving Optical SubAssemblies (MOSAs), which are mounted to a common static frame realizing the interface to the spacecraft structure (Figure 6). The rotation of each MOSA around an axis normal to the constellation plane is accomplished by an Optical Assembly Tracking Mechanism on the basis of a walking piezo motor. It is commanded as part of the DFACS loop on the basis of the DWS signals obtained on the science interferometer photodiodes, such that the local pointing is always referenced to the orientation of the wavefronts of the incoming beams.

2.2. Stray Light Mitigation

The realization of picometer level heterodyne detection for LISA requires the acquisition of optical phases at microcycle level accuracy, which might in general easily be harmed by already the slightest stray light interference on the photodiodes. Of particular concern in this context is stray light generated by the transmit beam in the optical path that it has in common with the receive beam, noting that the transmit power is about 1 W, while the total receive power is only about 200 pW. Several measures are taken to mitigate potential detrimental effects of such stray light.

The highest priority was given to the principal avoidance of any sources of stray light (in particular of

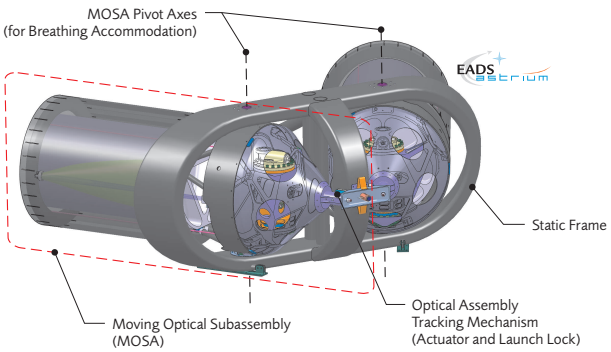

Figure 6. Baseline payload configuration with "Telescope Pointing", where line of sight steering is accomplished by rotating a rigid assembly of telescope, optical bench, and GRS.

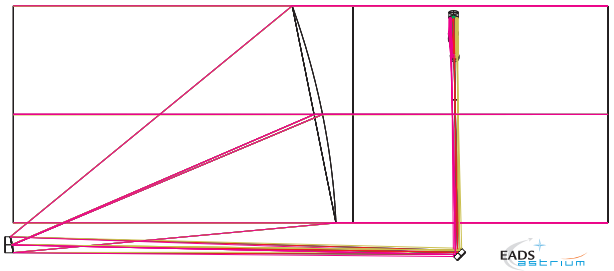

Figure 7. Narrow field off-axis telescope.

specular stray light) in the first place. This is accomplished by standard measures such as tilted optical surfaces, baffling, etc., but most notably by the use of a purpose-designed off-axis telescope, consisting of 2 mirrors and a 2 lens ocular, as schematically shown in Figure 7. A transmissive ocular was chosen as the most convenient solution in terms of manufacturing effort and accommodation, but it was nonetheless designed to fully suppress in-field specular back reflected light of the transmit beam. The design shows a wavefront error of better than $\lambda/100$ over the entire field of view of $\pm 350\,\mu$rad, as demonstrated by Figure 8.

In a secondary step, the use of orthogonal linear polarizations in transmit and receive beam, in combination with multiplexing of the two beams in a polarizing beam splitter, significantly attenuates any residual back reflections from the transmit beam into the receive path. A final suppression of potential stray light noise is achieved with a balanced receiver setup for the science interferometer, where the received light is mixed with laser radiation at the same frequency as the transmit beam. Such a "non-frequency-swap" configuration is principally insensitive to transmit beam stray light, unless one of the two receiver channels is lost due to failure. In this case, any potential impact of stray light on the science performance may still remain tolerable, as long as the scattering path is stable to about $1\,\text{nm}/\sqrt{\text{Hz}}$.

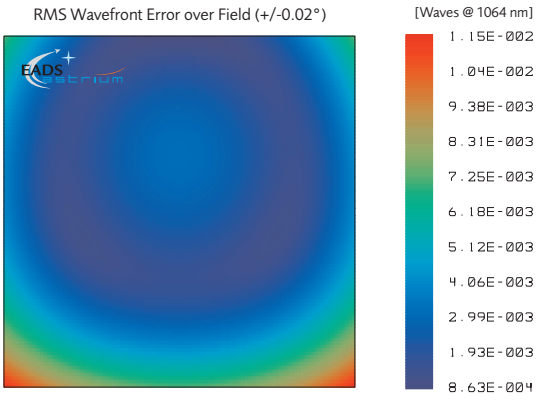

Figure 8. Design wavefront error over field for the baseline off-axis telescope.

Due to the necessity to provide picometer stability in the optical paths anyhow, the failure case can hence be handled as a redundancy fallback with graceful degradation.

In contrast, the occurrence of unexpected stray light in a "frequency-swap" configuration, where the received light is mixed with a third frequency (the local oscillator on the optical bench), might lead to a more severe performance degradation, if it starts saturating the first amplifier stage after the interferometer photodiode. On the other hand, such a setup offers the possibility to directly observe stray light, since it would generate a beat note separated in frequency from the main science beat note.

2.3. Pointing Jitter to Piston Crosstalk

As already addressed above, the optical pathlength effectively observed by the interferometric metrology system in LISA not only depends on the linear dimensions in the system, but is also affected by coupling of rotational degrees of freedom to the measurement path via geometrical projection. In consequence, it is necessary to also minimize or observe noise in the rotational degrees of freedom, typically to nanoradian level. For the strap-down architecture, the measurements to which geometrical projection applies are the local Optical Readout as well as the long arm science interferometry, for both of which the relevant fiducial point is the proof mass center of mass.

It is noted that geometrical projection effects not only result from actual geometrical offset of the respective line of sight from the fiducial points, but also from more indirect sources such as wavefront errors or an inhomogeneous distribution of the quantum efficiency over the active area of the photodiodes. The LISA measurement principle cannot distinguish between these sources, so that all of them can principally be characterized by a single "phase center offset" for each section of the strap-down chain.

For the long arm measurement, the noise budget is allocated such that the effective lateral phase center offset has to stay below 1.6 mm, assuming that the

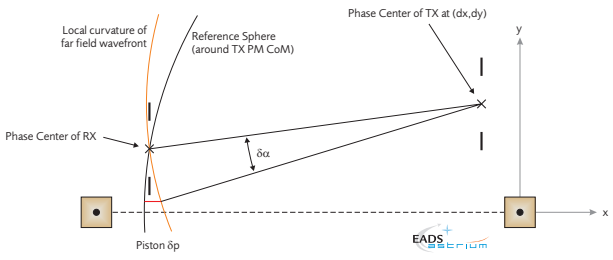

Figure 9. Geometrical interpretation of transmit phase center offset in the long arm interferometry.

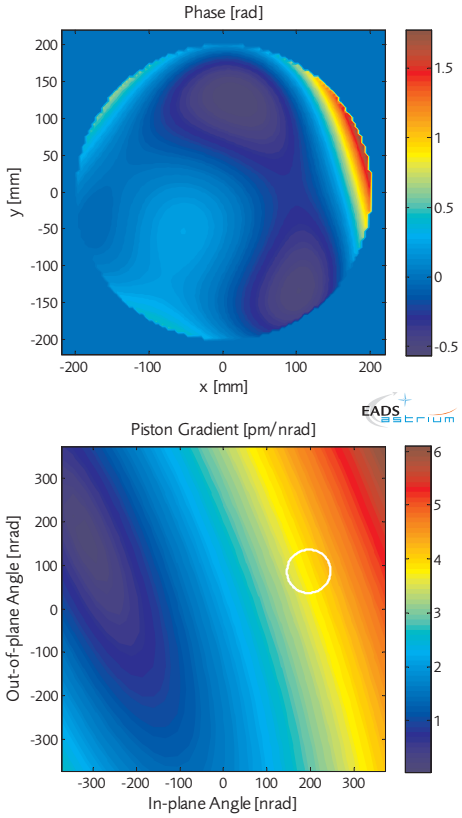

Figure 10. Far field gradient for a transmit wavefront error of $\lambda/18$ rms, distributed evenly over Zernikes Z_4 to Z_{11} according to Noll nomenclature. The white circle indicates the effective direction of observation. The top panel shows the phase distribution assumed in the transmit pupil.

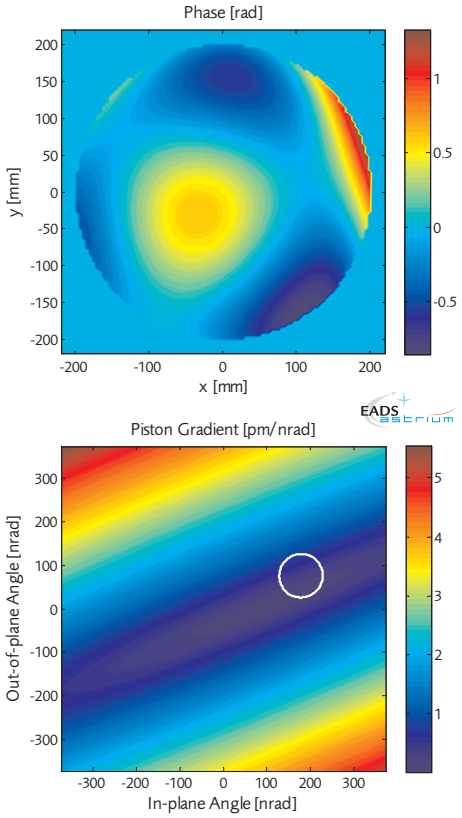

Figure 11. Phase distribution in the transmit pupil (top) and resulting far field gradient (bottom) after refocusing.

actual pointing can be determined to an accuaracy of $0.5\,\mathrm{nrad}/\sqrt{\mathrm{Hz}}$. Such an offset would manifest itself in a non-vanishing "far field gradient", i. e. a differential deviation of the far field wavefront from a perfect sphere, centered at the nominal proof mass center of mass of the transmitting spacecraft (Figure 9). The far field gradient $\partial\varphi/\partial\alpha$ couples to pointing jitter $\delta\alpha$ via

$$\delta p = \frac{\partial\varphi}{\partial\alpha}\cdot\delta\alpha \qquad (2)$$

to generate pathlength noise δp.

An example for the perturbation of the far field wavefront purely by wavefront errors in the transmit pupil is given in Figure 10. The simulation assumes an rms wavefront error of $\lambda/18$ in the 40 cm diameter exit pupil of the transmitting spacecraft, which is artificially generated by equally distributing this error over Zernikes Z_4 to Z_{11}, where the numbering is according to Noll. The piston gradient at the receiving spacraft for this case is 3.5 pm/nrad, and thus much larger than acceptable.

However, as shown in Figure 11, it is possible to correct the phase gradient at the point of observation by adjusting the focusing of the transmitted beam. In effect, this adds a curvature to the far field wavefront, which can locally compensate the errors generated by the other abberations in the optical system. Consequently, in order to provide a robust system with reasonable manufacturing effort, a refocusing capability is to be foreseen in the LISA telescope. It is currently realized by shifting one lens of the telescope ocular. A shift by ± 6 mm can change the focusing by the same amount that would result from a variation of $\pm 10\,\mu$m in the M1/M2 distance. Hence, the foreseen refocusing concept should be sufficient to both correct residual alignment errors and adjust the far field curvature at the operating point to the desired value.

Figure 12 finally demonstrates that equivalent effects can occur also on the science photodiodes due to aberrations in the receive path. For a perfectly flat receive wavefront, differential wavefront sensing would yield zero longitudinal signal if the wavefront is tilted around the center of the photodiode. As soon as abberations are present, however, the point of rotation leading to a longitudinal zero signal is significantly offset from the photodiode center, which in effect again corresponds to a potentially harmful phase center offset.

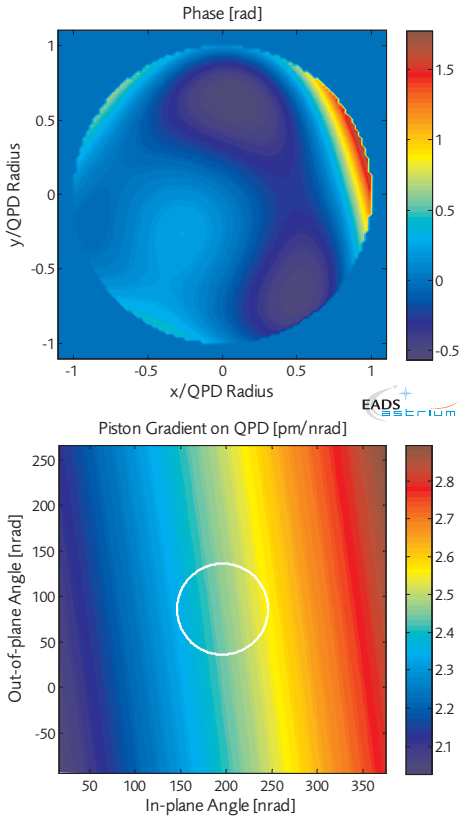

Figure 12. Effect of wavefront abberations at the receiving photodiode. The bottom panel shows the observed differential longitudinal signal in dependence of wavefront tilt, assuming wavefront errors as given in the top panel.

A second effect related to abberations in the receive path is the loss of heterodyne efficiency on the science receiver. On the basis of extensive simulation and analysis of the above effects for various kinds of wavefront errors, it is concluded that – if a refocusing capability is foreseen – it is in fact the constraints on the heterodyne efficiency that limit the tolerable wavefront errors in the optical system. In conclusion, allowing for a maximum wavefront error of about $\lambda/18$ rms in the optical system would yield a coherent solution, considering the combined constraints of far field gradient, refocusing capabilities, heterodyne efficiency, as well as QPD phase center offsets.

3. ANCILLARY METROLOGY

As part of the investigation of alternative payload configurations using In-Field Pointing, a variety of novel payload features have been introduced to improve the robustness of the mission against unexpected non-compliances in pathlength and/or pointing performance. In particular, ancillary metrology for monitoring of pathlength variations in the telescope subsystem and of PAAM pointing jitter have been developed, whose implementation is also considered to be beneficial for the present baseline design. It is stressed that currently neither feature is absolutely necessary to meet the required science performance.

Foreseeing a dedicated optical metrology system for the PAAM is motivated by the fact that residual pointing jitter of the PAAM has been one of the main factors limiting the achievable pointing knowledge. Improved pointing knowledge, in turn, would allow not only for a relaxation of tolerances on the phase center offsets, but also yield a higher accuracy for in-flight calibration procedures, for example. As discussed above, the implementation of such a metrology system is naturally compatible with locating the PAAM in the transmit path, and is realized with the same metrology principles already utilized anyhow on the optical bench (polarizing heterodyne interferometry and DWS).

The concept conceived for monitoring of potential pathlength fluctuations in the telescope, dubbed "Active Optical Truss", is depicted in Figure 13. It is based on the idea to directly refer the phase of the laser light leaving the spacecraft to the local optical bench reference frame. This is accomplished by picking off a small fraction of the transmitted beam at the height of M2, and mixing this light with a local oscillator delivered in free space directly from the optical bench. In consequence, the heterodyne signal will reflect any pathlength variations experienced by the transmit beam on its way from the optical bench to the telescope exit, independent of their source. On the other hand, it remains insensitive to any longitudinal motion of the optical truss detector assembly itself, since this would affect transmit and local oscillator paths in the same way.

To perfectly deduce the piston noise from the optical truss measurement, also dynamics in the wavefront

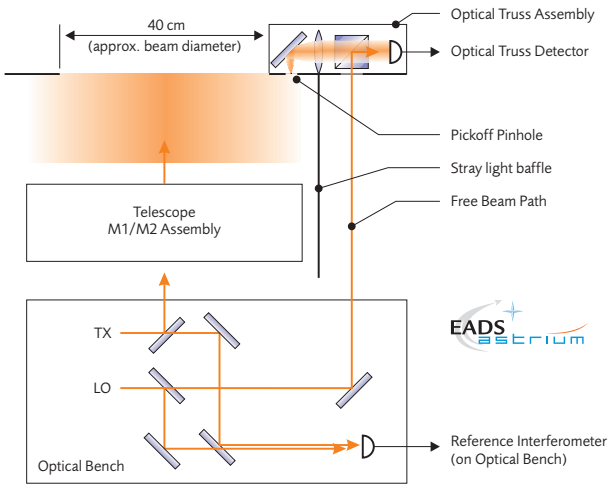

Figure 13. Concept of the active optical truss.

tilt at the telescope exit have to be monitored. For this purpose, a total of three optical truss detectors are arranged in a 120° configuration at the circumference of the transmit wavefront.

4. CONCLUSIONS

All of the issues, constraints, and specific features addressed above have been considered and merged into a novel opto-mechanical architecture of the LISA instrument in terms of the MOSA, which is detailed in Figure 14. Each MOSA comprises an off-axis telescope, an optical bench, and a Gravitational Reference Sensor containing the proof mass, which are isostatically attached to a central support ring.

Structural components, in particular the spacer between primary and secondary mirror, are designed to be made from ultra low expansion CFRP, in an approach to combine good optical pathlength performance with mechanical robustness. The optical bench baseplate employs Zerodur to provide sufficient dimensional stability for an adequate correlation of the individual interferometric measurements.

In addition to the basic science, reference, and Optical Readout interferometers, the optical bench includes the ancillary metrology functions described above (Figure 15). Furthermore, it houses a redundant sensor for initial beam acquisition and power monitor photodiodes. The transmitted beam is supplied by optical fiber from two laser systems operated in cold redundancy. Part of it is exchanged with the second optical bench on board via the backside fiber link, which thus provides the phase referencing between the two active lasers of each spacecraft.

In conclusion, we have matured the LISA opto-mechanical architecture over the past years into a self-consistent and robust baseline, for which no show stoppers have been identified.

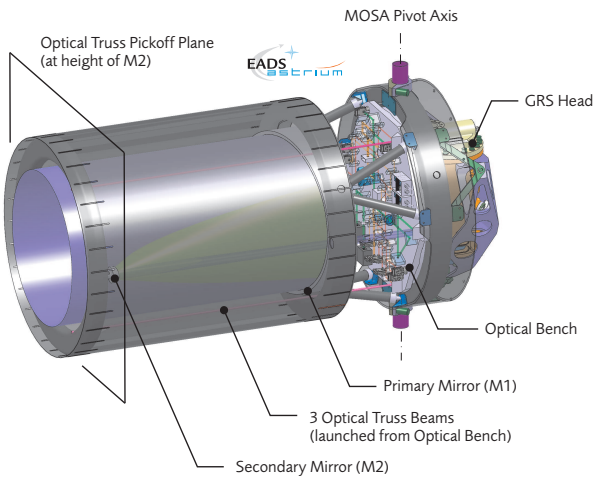

Figure 14. Moving Optical Subassembly (MOSA).

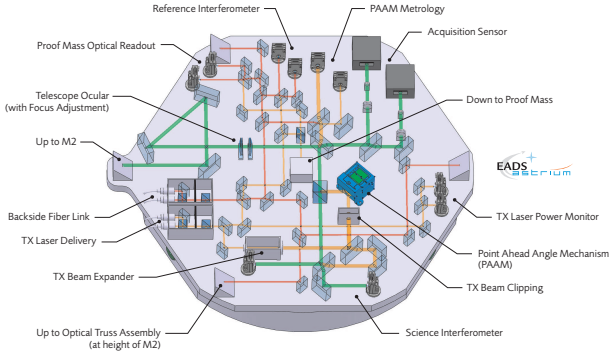

Figure 15. Optical bench layout.

ACKNOWLEDGMENTS

This work was supported by the European Space Agency under ESA Contract No. 18756/04/NL/HB. We further acknowledge the on-going fruitful collaboration with TNO (Delft) on the topic, as well as the always enlightening discussions within the ESA/NASA study group and with the LISA International Science Team (LIST).

REFERENCES

[1] D. Weise, C. Braxmaier, P. Gath, H. R. Schulte, and U. Johann. Optical metrology subsystem of the LISA gravitational wave detector. In A. Wilson, editor, *Proceedings of the Sixth International Conference on Space Optics*, 2006.

[2] E. Morrison, B. J. Meers, D. I. Robertson, and H. Ward. Automatic alignment of optical interferometers. *Applied Optics*, 33(22):5041, 1994.

[3] E. Morrison, B. J. Meers, D. I. Robertson, and H. Ward. Experimental demonstration of an automatic alignment system for optical interferometers. *Applied Optics*, 33(22):5037, 1994.